A phase-field approach for crack modelling of elastomers

Available online at www.sciencedirect.com

ScienceDirect

Procedia Structural Integrity 18 (2019) 694–702

Structural Integrity Procedia

www.elsevier.com/locate/procedia

25th International Conference on Fracture and Structural Integrity

A phase-field approach for crack modelling of elastomers

Roberto Brighenti[a,*], Andrea Carpinteri[a], Mattia Pancrazio Cosma[a]

[a]*Dept. of Engineering & Architecture – Univ. of Parma – Parco Area delle Scienze 181/A, 43124 Parma, ITALY*

Abstract

The description of a problem related to an evolving interface or a strong discontinuity requires to solve partial differential equations on a moving domain, whose evolution is unknown. Standard computational methods tackle this class of problems by adapting the discretized domain to the evolving interface, and that creates severe difficulties especially when the interface undergoes topological changes. The problem becomes even more awkward when the involved domain changes such as in mechanical problems characterized by large deformations. In this context, the phase-field approach allows us to easily reformulate the problem through the use of a continuous field variable, identifying the evolving interface (i.e. the crack in fracture problems), without the need to update the domain discretization. According to the variational theory of fracture, the crack grows by following a path that ensures that the total energy of the system is always minimized. In the present paper, we take advantage of such an approach for the description of fracture in highly deformable materials, such as the so-called elastomers. Starting from a statistical physics-based micromechanical model which employs the distribution function of the polymer's chains, we develop herein a phase-field approach to study the fracture occurring in this class of materials undergoing large deformations. Such a phase-field approach is finally applied to the solution of crack problems in elastomers.

Peer-review under responsibility of the Gruppo Italiano Frattura (IGF) ExCo.

*Keywords:*Elastomers; Fracture; Phase Field; Chains Distribution Function

Nomenclature

b	Kuhn's length of a chain segment
c_a	Number of active chain per unit volume

* Corresponding author. Tel.: +39 0521 905910; fax: +39 0521 905924.
E-mail address: brigh@unipr.it

2452-3216
Peer-review under responsibility of the Gruppo Italiano Frattura (IGF) ExCo.
10.1016/j.prostr.2019.08.217

f_0, f	Normalized distribution function of the polymer's chains end-to-end vector in the stress-free and in the current state, respectively
$\boldsymbol{F}, F_{ij}$	Deformation gradient tensor
G_c	Fracture energy
J	Material volume change, $J = \det \boldsymbol{F}$
k_B	Boltzmann's constant
$\mathcal{L}, \mathcal{L}^{-1}$	Langevin function and its inverse, respectively
N	Number of segments in a polymer chain belonging to a single network
p	Hydrostatic stress
$\boldsymbol{r}$	End-to-end distance of a polymer chain
$\boldsymbol{P}$	First Piola stress tensor
s	Order parameter or phase-field parameter
t	Time
$\boldsymbol{t}$	Force in a single chain
T	Absolute temperature
ϵ	Characteristic length of the phase field
$\varphi_0(\boldsymbol{r}), \varphi(\boldsymbol{r})$	Distribution function of the end-to-end vector in the stress-free and in the current state, respectively
λ	Stretch applied to the body and stretch of a polymer chain
ψ	Deformation energy in a single chain
$\Delta\Psi$	Network's deformation energy per unit volume
$\boldsymbol{\sigma}$	Cauchy stress
$\nabla(\blacksquare)$	Gradient operator

1. Introduction

Many real physical problems involve a moving boundary or interface, whose shape and position has to be determined while solving the problem itself. All these problems share the common feature that their mathematical description requires the solution of partial differential equations (PDEs) defined on a moving domain, coupled to others PDEs describing the boundary conditions on an evolving interface, Steinbach (2009); Miura (2018). Problems involving phase-change of a matter (liquid-solid-gas) as well as complex phenomena representing a transition from an undamaged to a fully broken material can be framed within this context.

The phase-field approach, originally developed to simulate microstructural evolution during solidification, Karma (2001), represents a tool that can be used to model a sharp transition from a phase to another one (Gomez & van der Zee (2018)). The main idea at the basis of this approach is to describe the two above-mentioned states through a so-called order parameter (phase-field variable) that represents a smooth transition between them. For instance, by considering the melting of matter, such a parameter may assume a value equal to 0 when the material is in a solid state and equal to 1 when the material is in a liquid state, varying smoothly from 0 to 1 during the transition, Karma (2001).

A similar concept can be applied in fracture mechanics: two states can be represented by the undamaged material and the ruptured one. According to the variational theory of fracture, the crack grows by following a path that ensures that the total energy of the system is minimized, Francfort & Marigo (1998). Within this approach, the total potential energy of the body is assumed to be provided by both the bulk strain energy of the material and the surface crack energy, the latter playing the role of the energy required for crack initiation and propagation, Ambati et al. (2015).

2. Statistical-based micromechanics of elastomers

2.1. Statistical description of the polymer's chains network

The mechanical response of an elastomer (or more generally of a polymer) is strictly connected to the state of its network, which is made of entangled chains joined together in several points called cross-links: every change of the network's configuration reflects on the macroscopic state of the elastomer. From this viewpoint, the knowledge of the effects produced on the network by any mechanism involved in the mechanical process allows us to evaluate the

deformation and the stress state of the polymer at the macroscale. The simplest microstructural model considers the polymer network to be made of chains, each one composed by a number N of rigid segments of equal length b, connected at their extremities and arranged according to the so-called random-walk theory, while no correlation is assumed to exist between the segments' directions (freely-jointed chain model, FJC), Treloar (1946); Fixman (1972); Boyce et al. (2000). According to the FJC model, the state of a polymer's chain is fully described by the knowledge of its chain' end-to-end vector $\boldsymbol{r}$; therefore, the statistical distribution of $\boldsymbol{r}$ provides the information required to evaluate the stress state of the material. Let us assume to represent the end-to-end vectors distribution by means of the function $\varphi(\boldsymbol{r})$, whose value for a given $\boldsymbol{r}$ gives us the number of network's chains having their end-to-end vector between $\boldsymbol{r}$ and $\boldsymbol{r}+\boldsymbol{dr}$. By using a classical Gaussian distribution (Doi (1966)), $\varphi(\boldsymbol{r})$ can be expressed by means of Eq.(1):

$$\varphi_0(\boldsymbol{r}) = \varphi(\boldsymbol{r}, t=0) = c_a \cdot f_0(\boldsymbol{r}) = c_a \cdot \left(\frac{3}{2\pi N b^2}\right)^{\frac{3}{2}} \exp\left(-\frac{3|\boldsymbol{r}|^2}{2Nb^2}\right) \tag{1}$$

being f_0 the dimensionless distribution and c_a the concentration of active chains, i.e. those involved in the bearing mechanism of the elastomer (dangling chains are neglected); since $r_0 = b\sqrt{N}$ is the average rest end-to-end vector length in the undeformed state (Doi (1996); Treloar (1946)) and, according to the affine deformation hypothesis $r = \lambda r_0$, with λ the current macroscopic deformation applied to the material, the statistical distribution of the chains can be also expressed as a function of the applied stretch as is reported in Eq.(2):

$$\varphi_0(\lambda) = c_a \cdot \left(\frac{3}{2\pi N b^2}\right)^{\frac{3}{2}} \exp\left(-\frac{3\lambda^2}{2}\right) \tag{2}$$

Following this approach, the mechanical behavior of an elastomer is governed by the evolution of its chains configuration, expressed by the function $\varphi(\lambda, t)$. Once the chains distribution is known, the potential energy per unit volume in the current (deformed) configuration is provided by the integral (evaluated over the chain configuration space) of $\Delta f(\boldsymbol{r}, t)$ (which is the difference between current distribution function and initial distribution function) times the energy of a single chain:

$$\Delta\Psi(t) = c_a \int_\Omega \Delta f(\boldsymbol{r}, t)\, \psi(\boldsymbol{r}) d\Omega, \qquad \Delta f(\boldsymbol{r}, t) = f(\boldsymbol{r}, t) - f_0(\boldsymbol{r}, 0) \tag{3}$$

The above integral has to be evaluated over Ω, i.e. over the whole chains configuration space, Vernerey et al. (2017). The energy stored in a single chain $\psi(\boldsymbol{r})$ can be evaluated by using the Langevin statistics (which is valid for moderate and large deformations), according to which $\psi(\boldsymbol{r}) = N k_B T \cdot \left(\frac{\beta}{bN}\boldsymbol{r} + \ln\frac{\beta}{\sinh\beta}\right)$, where $\beta = \mathcal{L}^{-1}\left(\frac{r}{bN}\right) = \mathcal{L}^{-1}\left(\frac{\lambda}{\sqrt{N}}\right)$ (being $\mathcal{L}^{-1}(\blacksquare)$ the inverse of the Langevin function, $\mathcal{L}(\blacksquare) = \coth(\blacksquare) - \blacksquare^{-1}$), with k_B and T the Boltzmann's constant and the absolute temperature, respectively, see Treloar (1946).

2.2. Stress state in the material

Once the potential energy of the material's is known (Eq.(3)), the stress is obtainable through the following derivative of the free energy with respect to the deformation gradient ($\boldsymbol{F}$), Vernerey et al. (2017), Brighenti et al. (2019):

$$\boldsymbol{\sigma} = J^{-1}\boldsymbol{P}\boldsymbol{F}^T = J^{-1}\left[\frac{\partial\Delta\Psi(t)}{\partial\boldsymbol{F}} + Jp(t)\boldsymbol{F}^{-T}\right]\boldsymbol{F}^T \tag{4}$$

being $\boldsymbol{\sigma}$ and $\boldsymbol{P}$ the Cauchy and the first Piola stress tensors, respectively. Further, p is the hydrostatic pressure required to enforce the polymer's incompressibility condition typically adopted, that mathematically reads $J = \det\boldsymbol{F} = 1$. By

rearranging the previous expression, after some calculations and by using the force existing in the chains expressed as $\boldsymbol{t} = d\psi/d\boldsymbol{r}$, the Cauchy stress can be more conveniently expressed as follows:

$$\boldsymbol{\sigma} = \int_{\Omega} (\varphi - \varphi_0)[\boldsymbol{t} \otimes \boldsymbol{r}] d\Omega + p\mathbf{1} \tag{5}$$

3. Basic concepts of the phase-field approach in fracture mechanics

3.1. Theoretical aspects of the phase-field in fracture mechanics

The phase-field approach in fracture mechanics originates from the variational formulation of brittle fracture proposed by Franckfort & Marigo (1998). This approach provides the solution of the fracture problem by minimizing the following energy functional:

$$\Pi = \int_{\mathcal{B}} \Delta\Psi(\boldsymbol{r}, t) dV + G_c \int_{\Gamma_c} dA = \Pi_b + \Pi_s \tag{6}$$

where $\Delta\Psi$ and G_c are the internal energy per unit volume of the material and the fracture energy per unit area, respectively. It is worth mentioning that the first integral in Eq. (6) is performed over the current domain of the body ($\mathcal{B}$), whereas the second one is an integral to be evaluated over the current crack domain (Γ_c), which is generally not known and has to be determined by solving the fracture problem, Ambati et al. (2015). The phase-field approach operates by regularizing the crack domain (diffuse crack), in order to compute the energy functional (Eq. (6)) by integrating both terms over $\mathcal{B}$. This regularization consists in introducing an approximate smooth description of the physical discontinuity, characterized by a so-called (small) length parameter ϵ; the real sharp crack in the body is exactly recovered only when the length parameter tends to zero, $\epsilon \to 0$.

Let us assume that the body in its undeformed configuration occupies the region $\mathcal{B}_0 \subset \mathcal{R}^{\mathrm{d}}$, d being the dimension of the space ($d = 1, 2, 3$), whereas $\partial\mathcal{B}_0$ represents the boundary of $\mathcal{B}_0$. The body is assumed to contain a sharp discontinuity $\Gamma_{c0} \subset \mathcal{R}^{d-1}$ that, for a fracture process, represents the crack line or the crack surface depending on the dimension of the problem. Obviously, our case being an elastomer prone to large deformations, the current domains of the body and of the crack $\mathcal{B}$, Γ_c can be different from the corresponding ones in the undeformed state, $\mathcal{B}_0$, Γ_{c0}. The above mentioned regularization is performed by introducing an auxiliary field variable $s(\boldsymbol{X}, t)$; it can take values in the range $0 < s \leq 1$, where the value $s = 0$ indicates the solid (or undamaged) material while $s = 1$ represents the cracked (fully damaged) one. Since a smoothly transition has been introduced, also intermediated values exist in a region close to the crack, indicating a transition between the failed ($s \to 1^-$) and the unfailed ($s = 0^+$) material. The field map of the phase-field parameter provides an approximate (diffused) description of the actual crack (Fig. 1).

By means of the adopted regularization, the energy functional in Eq. (6) can be reformulated by following Miehe et al. (2010):

$$\Pi = \int_{\mathcal{B}} g(s)\, \Delta\Psi(\boldsymbol{r}, t) dV + \frac{G_c}{2\epsilon} \int_{\mathcal{B}} s^2 + \epsilon^2 |\nabla s|^2 dV = \widetilde{\Psi}_b + \Psi_s \tag{7}$$

It can be noticed that the internal energy of the material $\Delta\Psi(\boldsymbol{r}, t)$ in Eq.(7) is multiplied by the function $g(s) = [(1 - s)^2 + \eta]$, that represents the energy degradation of the material when it is fully broken or near to be fully broken ($s \to 1$); the term η in $g(s)$ is a small number providing a residual stiffness when the material is completely failed, and it is required to avoid numerical drawbacks. The second integral represents the energy of fracture, where G_c is the material's fracture energy.

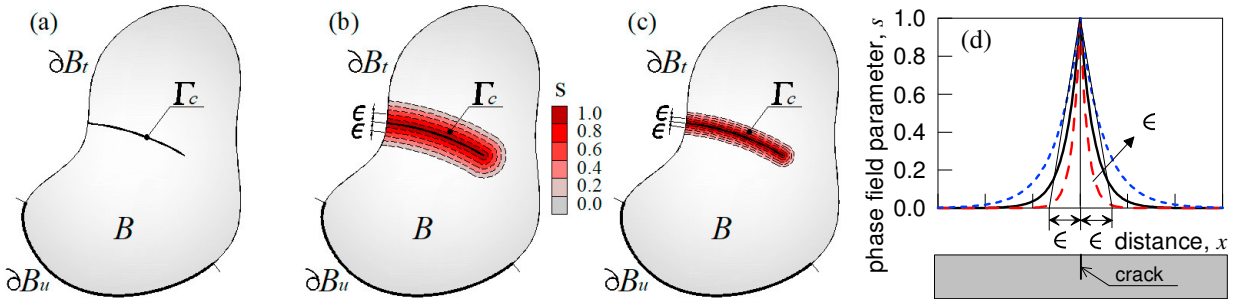

Fig. 1. (a) Sharp crack Γ_c embedded in the solid $\mathcal{B}$; (b-c) diffused representation of the crack for two different values of the length parameter ϵ. (d) One dimensional cracked element example: phase field representation of the crack for different values of ϵ.

As is recalled above, since the system physically evolves in such a way to minimize its internal energy, the crack grows by following a path that ensures that the total energy is always minimum; the governing equations of the problem can be deduced by minimizing the functional of Eq.(7), leading to (Miehe et al., 2010):

$$[(1-s)^2+\eta]\mathrm{Div}\boldsymbol{P}+\boldsymbol{B}=\boldsymbol{0} \qquad \text{in } \mathcal{B}_0 \tag{8}$$

$$2(s-1)\Delta\Psi+G_c\left(\frac{s}{\epsilon}-\epsilon\nabla^2 s\right)=0 \qquad \text{in } \mathcal{B}_0 \tag{9}$$

where $\boldsymbol{B}$ is the vector of body forces. The above governing equations must be equipped with the corresponding boundary conditions:

$$\boldsymbol{u}=\overline{\boldsymbol{u}} \qquad \text{in } \partial\mathcal{B}_{0u} \tag{10a}$$

$$[(1-s)^2+\eta]\boldsymbol{F}\boldsymbol{S}\boldsymbol{n}=\overline{\boldsymbol{T}} \qquad \text{in } \partial\mathcal{B}_{0T} \tag{10b}$$

$$\nabla s\boldsymbol{n}=0 \qquad \text{in } \partial\mathcal{B}_0 \tag{10c}$$

where $\overline{\boldsymbol{T}}$ represents the vector of the traction forces and $\boldsymbol{n}$ is the unit outward normal to the boundary of the undeformed domain of the body.

Because of the material degradation at or close to the crack location, the degradation function $g(s)$ has to be applied also to the stress field. In fact, as the damage of the material developes, the loss of elastomer's stiffness reflects on the relaxation of the stress state, implying that the stress has to be reduced according to the order parameter quntified by the phase field in the material. Mathematically this is provided by:

$$\tilde{\boldsymbol{\sigma}}=[(1-s)^2+\eta]\cdot\left\{\int_\Omega(\varphi-\varphi_0)[\boldsymbol{t}\otimes\boldsymbol{r}]d\Omega+p\boldsymbol{1}\right\} \tag{11}$$

3.2. FE numerical implementation of the phase-field

The numerical solution of the above stated problem, can be determined by implementing the governing equations (Eqs (8)-(10)) in a standard finite element setting; the involved standard fields (displacements, deformations, etc.) and the new ones (phase-field and phase-field gradient) have to be discretized through the interpolation of the corresponding nodal values, i.e.:

$$\begin{aligned} \overline{\boldsymbol{u}} &= \sum_{i=1}^{n_n} [N]_i \, \boldsymbol{u}_i, \quad \overline{\boldsymbol{F}} = \mathbb{I} + \sum_{i=1}^{n_n} [B_u]_i \boldsymbol{u}_i, \\ \bar{s} &= \sum_{i=1}^{n_n} N_i \, s_i \, , \qquad \nabla \bar{s} = \sum_{i=1}^{n_n} [B_s]_i s_i \end{aligned} \tag{12}$$

where the upperbar terms are the element's interpolated vector or scalar quantities, n_n represents the number of nodes of the element, u_i, s_i are the nodal displacements and the nodal values of the phase-field parameter, respectively, while N_i is the shape function associated to the $i-th$ node of the element, B is the compatibility matrix containing the derivatives of the shape functions, and $\mathbb{I}$ is the identity matrix. In a 2D setting, each element's node is characterized by three degrees of freedom, i.e. two displacements and the phase field values. The non-linear governing equations (8)-(9), corresponding to the equilibrium and the phase-field evolution, can be linearized and the problem can be solved incrementally:

$$\boldsymbol{K}_T \begin{Bmatrix} \Delta \overline{\boldsymbol{u}} \\ \Delta \bar{s} \end{Bmatrix} = - \begin{Bmatrix} \boldsymbol{R}_u \\ R_s \end{Bmatrix} \tag{13}$$

where $\boldsymbol{K}_T = \begin{bmatrix} \frac{\partial \boldsymbol{R}_u}{\partial \boldsymbol{u}} & \frac{\partial \boldsymbol{R}_u}{\partial s} \\ \frac{\partial \boldsymbol{R}_s}{\partial \boldsymbol{u}} & \frac{\partial \boldsymbol{R}_s}{\partial s} \end{bmatrix}$ is the tangent stiffness matrix, while the residual vectors $\boldsymbol{R}_u$, $\boldsymbol{R}_s$ are deduced by assembling the corresponding elements' residual vectors $\boldsymbol{R}_{\boldsymbol{u}}^e$, $\boldsymbol{R}_s^e$ (Miehe et al;. 2010):

$$\begin{aligned} \boldsymbol{R}_{\boldsymbol{u}}^e &= \int_{\mathcal{B}_{0,e}} [(1-N_i s_i)^2 + \eta][B_u]_i^T \boldsymbol{P} dV - \left(\int_{\mathcal{B}_{0,e}} N_i^T \boldsymbol{B} dV + \int_{\partial \mathcal{B}_{0,e}} N_i^T \overline{\boldsymbol{T}} dA \right) \\ \boldsymbol{R}_s^e &= \int_{\mathcal{B}_{0,e}} \tilde{G}_c \epsilon [B_s]_i^T \, \nabla s + \left(\frac{G_c}{\epsilon} + 2 N_i \Delta \Psi_i \right) N_i s_i dV - \int_{\mathcal{B}_{0,e}} 2 N_i \Delta \Psi_i \, dV \end{aligned} \tag{14}$$

In the evaluation of the phase field evolution, the energy density $\Delta \Psi$ at a given time instant t' has to be considered as a state parameter defined as $\Delta \Psi(t') = \max_{t<t'} \Delta \Psi(t)$ in order to guarantee the irreversibility of the fracture process. Moreover, it is worth mentioning that the phase field approach operates on a fixed mesh and, therefore, no remeshing operations during crack propagation are needed, thus providing an important advantage with respect to other computational techiques developed for fracture problems.

3.3. Fracture energy of elastomers: from micro-scale to macro-scale

As is illustrated in Sect. 2, what happens to the network of the elastomer's chains reflects on the macroscopic behavior at the continuum level; similarly, the macroscopic fracture process can be related to the failure of the single chains composing the polymer network. In other words, since we developed the phase field approach to study the fracture process in polymers on the basis of a statistical-based micromechanical model, the macroscopic fracture energy G_c of the material must be evaluated on the basis of the failure mechanisms taking place at the chains level.

Typically, an elastomer is made by long linear entangled chains, each one constituted by the repetitions of monomer units jointed together by $C-C$ chemical bond. This observation suggests that the rupture of a polymeric chain corresponds to the dissociation of the primary $C-C$ bond; therefore, we could try to relate G_c to the chemical bond strength energy of dissociation. However, an evaluation of the fracture energy simply obtained as the ratio between the bond strength and the cross sectional area of the monomer unit leads to values that are less than one-twentieth of the effective G_c obtained from experimental tests.

This happens because all the monomer units and the entangled chains work collectively to bear the external load, and this mechanism justifies the measures values of the fracture energy to be greater than the dissociation energy per unit area of a single bond.

To relate G_c to the micro scale failure mechanism, we use a simple model developed by Lake et al. (1967), schematically shown in Fig. 2. Let us consider a chain lying between adjacent crosslinks, having mean end-to-end distance r_0, and containing N monomer units (no. of Kuhn segments); U is the energy to break a monomer unit, while the energy required to break the whole chain can be approximated as $N \cdot U$.

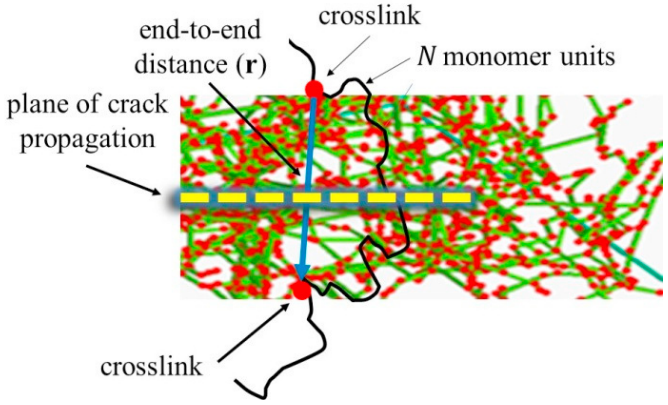

Fig. 2. Scheme of a polymer chain lying across the plane of crack propagation.

By considering a polymer chain crossed by the plane of crack propagation (see Fig. 2), G_c is determined multiplying the energy required to break a single chain by the number of chains crossing a unit cracked area, $n_\Gamma = \frac{1}{2} r_0 n$, where $n = c_a = \frac{\mu}{k_B \cdot T}$ represents the number of chains per unit volume and μ is the shear modulus of the material. Finally, the value of G_c can be estimated as follows (Lake et al. (1967); Miehe et al. (2014)):

$$G_c = n_\Gamma \cdot N \cdot U = \frac{1}{2} \cdot b \cdot \frac{\mu}{k_B \cdot T} \cdot N^{3/2} \cdot U \tag{15}$$

where the rest end-to-end distance of the chain has been expressed as $r_0 = b\sqrt{N}$.

4. Numerical examples

The phase field approach presented above is herein applied to the solution of a fracture problem: a rectangular plate with dimensions $W \times 2L \times t$ (thickness) is restrained at its bottom edge and is loaded by a force P applied to its upper edge's midpoint through a rigid element connected to the same edge (Fig. 3). The plate contains an initial straight edge crack of length $a/W = 0.3$, whereas the geometrical ratios of the plate are $L/W = 1.2$ and $t/W = 0.1$. The material is assumed to be in plane stress condition and is characterized by the following mechanical properties: elastic modulus $E = 20\text{MPa}$, Poisson's ratio $\nu = 0.495$. The case of an elastic-perfectly brittle material is examined (two fracture energies are adopted, $G_c = 10\ \text{N/m}$ and $G_c = 30\ \text{N/m}$) as well as the case of an elastic polymer having the same mechanical properties; in the latter case the mechanical response of the material is obtained on the basis of the statistical-based approach presented in the previous sections. Finally, the phase field calculation has been performed by using a staggered solution scheme, i.e. by solving alternatively the mechanical and the phase field evolution problems (Hofacker & Miehe (2012); Huynh et al. (2019)), the latter problem solved by adopting the length parameter equal to $\epsilon/W = 0.05$. Large displacement nonlinearity is accounted for, while no strain rate effects are taken into account for the mechanical response simulated through the computational approach illustrated above.

In Fig. 3a the scheme of the examined plate under deformation is illustrated; Figs 3b, c display the dimensionless stress σ_0/E (nominal remote stress evaluated as $\sigma_0 = P/(W \times t)$) vs the dimensionless vertical displacement s_y/W of the central top point of the plate for both the elastic-brittle material (Fig. 3b) and the polymeric one (Fig. 3c), for the two fracture energy values analysed. In the same figures, some plate's configurations are identified with the letters A1, A2,…, D3, and the corresponding crack patterns are illustrated in Fig. 4.

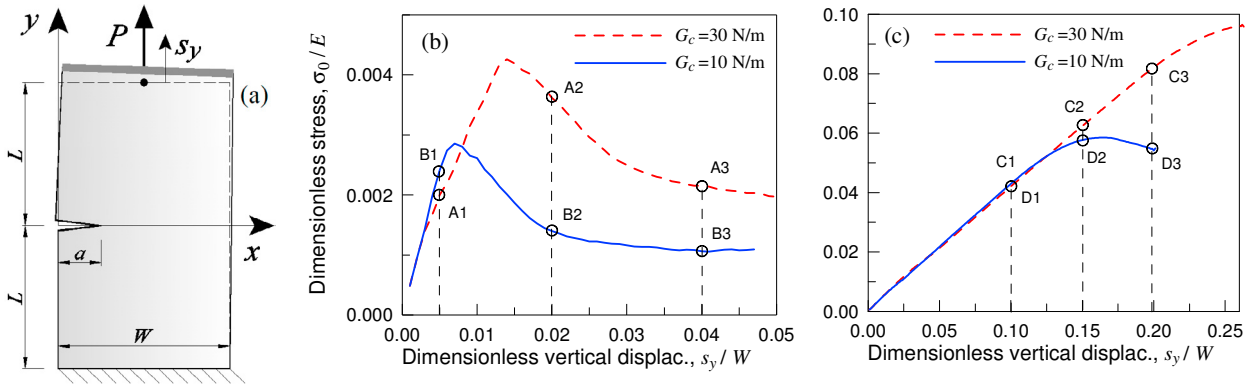

Fig. 3. (a) Edge cracked plate under a tensile force P. (b) Dimensionless load vs dimensionless displacement for the elastic-brittle plate and (c) for the polymeric one, for two values of the fracture energy.

The response of the elastic-brittle plate is characterized by a noticeably softening branch because of the brittleness of the material; by increasing the fracture energy the peak stress increases as is expected (Fig. 3b). On the other hand, for the polymeric plate the response is quite different since the behavior is ductile, and no clear peak stress can be identified except the case with the lowest fracture energy (Fig. 3c).

Correspondingly, the crack patterns developed in the plate are shown in Fig. 4 for the states marked in Fig. 3; being the plate under a point load applied through a rigid straight element lying on the top edge of the plate (Fig. 3a), the fracture process is not in pure Mode I, but also Mode II appears.

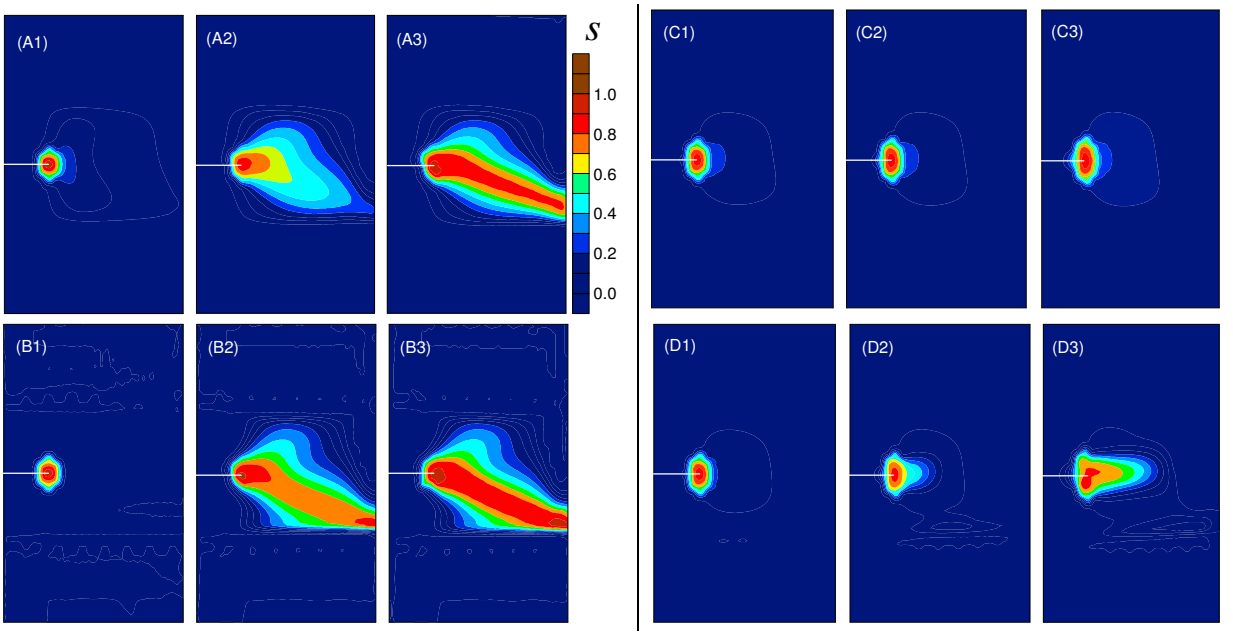

Fig. 4. Crack patterns corresponding to the states indicated in Fig. 3b, obtained from the phase field approach for the elastic-brittle plate with fracture energy $G_c = 30$ N/m (A1, A2, A3) and $G_c = 10$ N/m (B1, B2, B3). Crack patterns corresponding to the states indicated in Fig. 3c, for the polymeric plate with fracture energy $G_c = 30$ N/m (C1, C2, C3) and $G_c = 10$ N/m (D1, D2, D3).

The crack paths determined through the phase field clearly indicate the crack propagation in mixed mode, especially for the elastic-brittle material (crack patterns indicated on the left-hand side of Fig. 4), while the crack patterns for the polymeric material, which responds in a much more ductile way, are less developed indicating that the plate is much more defect-tolerant as is well-known from the literature (Yuan et al. (2010); Brighenti et al. (2017)).

5. Conclusions

Because of the discontinuous nature of mechanical problems involving the development of cracks, the so-called phase-field approach has been developed, based on the variational theory of fracture, by representing the damaged (cracked) material through a smooth continuous function. In the present paper, we have adopted such an approach to study the fracture of polymeric materials, whose mechanical behavior has been described by a micromechanical model accounting for both their large deformations and incompressibility feature. The macroscopic fracture energy has also been estimated on the basis of the polymer's chains properties.

The micromechanical model has been combined with a phase field approach for fracture simulation, and its implementation into a finite element framework has been described. The simulations performed through the developed approach have shown that the effectiveness of the phase field to solve complex fracture problems without any need of particular intervention during the analysis, such as the remeshing or the use of cohesive elements. Different constitutive models can be adopted for the material within the phase field approach; in this paper both elastic-brittle materials and polymeric materials are examined and simulated by the developed computational tool. The higher defect tolerance of polymeric materials with respect to traditional linear elastic ones has been shown for quasi static fracture problems under large deformations.

References

Ambati, M., Gerasimov, T., Lorenzis, L., 2015. A Review on phase-field models of brittle fracture and a new fast hybrid formulation. Comput. Mech. 55, 383–405.

Brighenti, R., Carpinteri, A., Artoni, F., 2017. Defect sensitivity to failure of highly deformable polymeric materials. Theor. Appl. Fract. Mech. 88, 107–116.

Brighenti, R., Artoni, F., Cosma, M.P., 2019. Mechanics of materials with embedded unstable molecules. J. Sol. Struct. 162, 21–35.

Boyce, M., Arruda, E., 2000. Constitutive models of rubber elasticity: a review, Rubber Chem. Tech., 73.3, 504–523.

Doi, M., 1996. Introduction to polymer physics. Oxford university press.

Fixman, M., 1972. Modern theory of polymer solutions. Hiromi Yamakawa. Harper and Row, New York, 1971, Harper's Chemistry Series.

Francfort, G.A., Marigo, J.J., 1998. Revisiting brittle fracture as an energy minimization problem. J. Mech. Phys. Sol. 46(8), 1319–1342.

Gomez, H., van der Zee, K.G., 2018. Computational phase-field modeling. Encyclopedia of Computational Mechanics Second Edition, 1-35.

Hofacker, M., Miehe, C., 2012. Continuum phase field modeling of dynamic fracture: variational principles and staggered FE implementation. J. Fract. 178(1-2), 113-129.

Huynh, G.D., Zhuang, X., Nguyen-Xuan, H., 2019. Implementation aspects of a phase-field approach for brittle fracture. Frontiers of Struct. Civil Eng. 13(2), 417-428.

Karma, A., 2001. Phase-field formulation for quantitative modeling of alloy solidification. Phys. Rev. Lett. 87, 115701.

Lake, G.J., Thomas, A.G., Tabor, D., 1967. The strength of highly elastic materials. Proceedings of the Royal Society of London. Series A. Math. Phys. Sci. 300, 108–119.

Miehe, C., Welschinger, F., Hofacker, M., 2010. Thermodynamically consistent phase-field models of fracture: Variational principles and multi-field FE implementations. J. Num. Meth. Eng. 83(10), 1273-1311.

Miehe, C., Schänzel, L.M., 2014. Phase field modeling of fracture in rubbery polymers. Part I: Finite elasticity coupled with brittle failure. J. Mech. Phys. Sol. 65, 93-113.

Miura, H., 2018. Phase-field model for growth and dissolution of a stoichiometric compound in a binary liquid. Phys. Rev. E 98(2), 023311.

Steinbach, I., 2009. Phase-field models in materials science. Model. Simul. Mat. Sci. Eng. 17(7), 073001.

Treloar, L.R.G., 1946. The elasticity of a network of long-chain molecules.— III. Trans. Faraday Soc. 42, 83–94.

Vernerey, F.J., Long, R., Brighenti, R., 2017. A statistically-based continuum theory for polymers with transient networks. J. Mech. Phys. Sol. 107, 1–20.

Yuan, W., Li, H., Brochu, P., Niu, X., Pei, Q., 2010. Fault-tolerant silicone dielectric elastomers. J. Smart Nano Mat. 1(1), 40-52.